Diffusion of Uncharged Solutes Through Human Nail Plate

Sudhir M. Baswan, **S. Kevin Li**, and **Gerald B. Kasting**[*]

James L. Winkle College of Pharmacy, The University of Cincinnati Academic Health Center

Abstract

Passive diffusion data for uncharged solutes in hydrated human nail plate are collected and compared to the predictions of two theories for diffusion of uncharged solutes in dense keratin matrices. Quantitative agreement between the experimental data and the theories examined is poor. Concerns with both the experiments and the theories are identified and discussed. It is evident from the analysis that magnitude of the experimental nail permeability data may be questioned, as may the extrapolation procedures used to estimate the properties of dense fiber arrays from more dilute systems. Despite these caveats, it can be inferred that the microstructure of the nail plate is more complex than that assumed in the described models. The influence of residual lipids is implicated. More rigorous experiments and theoretical analysis of mass transport in the nail plate system are warranted. Successful completion of these tasks could lead not only to better predictions of transungual drug delivery, but also to better models of skin permeability, if hydrated nail plate can indeed serve as a model for the corneocyte phase of (partially hydrated) stratum corneum.

Keywords

onychomycosis; passive diffusion; fiber matrix model; transungual drug delivery; nail permeability; corneocyte permeability

1. Introduction

It has been frequently stated that human nail plate (1), and also horny tissues derived from other sources (2), behave as hydrogels with respect to passive diffusion. Were this the case, and considering the large body of literature available on diffusion through hydrogels and other fiber matrix systems (3), it would seem that diffusion through nail should therefore be predictable. The catch is that the nail matrix is a very concentrated system, with fiber volume fraction ranging from approximately 0.64 for fully hydrated nail (4, 5) to 0.78 for partially hydrated nail (6), whereas most hydrogel diffusion theories deal with dilute systems. Additional complications involve the charge state of the matrix (which varies with pH), the complex and not completely known orientation of the keratin microfilaments (7) and the possible involvement of residual lipids in the diffusion barrier (8).

[*]**Correspondence**: Gerald B. Kasting, James L. Winkle College of Pharmacy, The University of Cincinnati Academic Health Center, P.O. Box 670004, Cincinnati, Ohio 45267-0004, Phone: (513) 558-1817, Fax: (513) 558-0978, gerald.kasting@uc.edu.

In this report we assemble available passive diffusion data for small uncharged solutes traversing hydrated human nail plate and compare the results with two fiber matrix theories developed for skin corneocytes, which have a fiber volume fraction of about 0.64 when in their partially hydrated state (9). Keratin microfibril orientation in both nail and stratum corneum is thought to be predominately in the plane of the membrane so, at comparable fiber densities, the comparison seems relevant. In order to avoid the complications introduced by electrostatic interactions, the present analysis is confined to uncharged solutes. It will be seen that neither of the theories tested matches the experimental in vitro permeability data in nail. But there are also unresolved questions regarding the data. The analysis suggests that a careful study of nail ultrastructure, a confirmatory permeability study and a rigorous calculation of mass transport in this system are warranted.

2. Method

Data collected from the literature were subjected to the following inclusion criteria in order to limit the variability in the database: (a) the data were reported for human nail plate; (b) the experiments were conducted in either aqueous solutions or ethanol/water mixtures with no additional permeation enhancers; and (c) the data were reported in terms of permeability coefficients ($k_p = J_{ss}/\;C = DK/h$) or k_p could be calculated from the provided information. If the experimental k_p values were obtained at temperatures other than 32°C, a temperature correction factor derived from the solution viscosity ratio was used to correct k_p values to $k_p{}'$. The correction factors for experiments performed at 20, 25 and 37°C were calculated to be 1.365, 1.192 and 0.890, respectively. The reported k_p' values were normalized by the thickness of the nail sample, h, to yield specific permeability, $P = D\cdot K$. Experimental values of nail thickness were used for each solute when available; otherwise the average value provided by the source was employed. In cases where no data on nail thickness were reported, a value of 0.05 cm was used. Molar volume at the normal boiling point, V_m, was calculated according to Schroeder's method (10) and the diffusivity in aqueous solution D_0 was estimated from the Wilke-Chang correlation (9). Solute radius, R_s, was calculated from V_m using Equation 1:

$$R_s = 0.155123 V_m^{0.6} \quad (1)$$

This relationship yields the hydrodynamic radius of the solute, i.e. the radius that when inserted into the Stokes-Einstein relationship yields the correct value of D_0 (9). The proportionality constant in Equation 1 differs from that given in (9) due to the fact that the solvent association factor of 2.26 for water recommended by Hayduk and Laudie (11) has been employed in lieu of the original Wilke-Chang value of 2.6. The physicochemical properties, permeability coefficients, aqueous diffusivities and specific permeabilities for 42 uncharged solutes in nail plate are listed in Table 1. The ratio P/D_0 was calculated to provide a point of comparison with current theories of transport in dense keratin matrices. This quantity may be seen to be the extent to which solute diffusion through the matrix is altered with respect to diffusion in water.

The theories discussed include one from our own extended group (9, 12) and one offered by workers at China Agricultural University (13). They will be referred to as the UB/UC and CAU models, respectively. A more thorough comparison is given elsewhere (14). The UB/UC model derives from calculations for cylindrical fibers randomly oriented in a plane perpendicular to the direction of diffusion conducted for large solutes at low fiber densities by Phillips et al. (15). The rigorous calculations described therein were limited to $0.5 < \lambda < 5$, where $\lambda = r_s/r_f$ is the ratio of solute to fiber radii and (for $\lambda = 0.5$) to fiber volume fractions $\phi_f < 0.17$. They were extrapolated to the limit $\phi_f = 0.60$ for small solutes in partially hydrated corneocytes as described in (9) and more thoroughly for $\phi_f = 0.64$ in (9, 12). The CAU model derives from work by Johnson et al. on macromolecules diffusing in agarose gels (16), another very dilute fiber system. Chen et al. (13) fit the two parameters α and β in the Johnson et al. model in order to match steady-state permeability data of eight solutes in human stratum corneum. Such a procedure implicitly implies that diffusion through the protein matrix is the rate-limiting step in transport through the SC. We note that both models were developed for uncharged solutes traversing uncharged membranes. Electrostatic interactions were not considered. Consequently, we have limited the present comparison to uncharged solutes which should not be strongly impacted by the net negative charge on the nail keratin matrix. The governing relationships for both the UB/UC and CAU models are given in Appendix 1. We wish to emphasize that the effect of hydration on nail permeability is taken into account in both models through the fiber volume fraction parameter, ϕ_f.

3. Results and Discussion

Plots of $\log k_p'$ versus $\log K_{o/w}$ (Fig. 1a) and $\log k_p'$ vs.log MW (Fig. 1b) for the data in Table 1 reinforce the findings of Kobayashi et al. (1): there is a strong inverse dependence of $\log k_p'$ on log MW, but no apparent dependence of $\log k_p'$ on $\log K_{o/w}$. These statements are supported by linear regressions on these data:

$$\log k_p' = -6.84 - 0.02 \log \mathrm{K_{o/w}} \quad (2)$$

$$n=38, s=0.72, r^2=0.004$$

$$\log k_p' = -3.11 - 1.75 \log \mathrm{MW} \quad (3)$$

$$n=38, s=0.41, r^2=0.68$$

Four compounds (decanol, dodecanol, flurbiprofen and ketoprofen) were excluded from the analysis for reasons discussed later. It should be noted that Equation 3 explains 68% of the

variance in the log k_p' data and leads to a standard deviation $s = 0.41$; thus, Equation 3 predicts the k_p' data to within a root mean square factor of $10^{0.41}$ or about 2.6.

Of greater interest for this report was the comparison of the normalized nail plate permeability P/D_0 with predictions of the UB/UC and CAU models (Fig. 2). The UB/UC model overestimated the normalized nail permeability data whereas the CAU model severely underestimated it. A linear regression on log P/D_0 vs. R_s, from which the four outlying data were excluded, yielded

$$\log P/D_0 = -1.70 - 0.40 R_s \quad (4)$$

$$n = 38, s = 0.40; r^2 = 0.57$$

The lower r^2 value for Equation 4 as compared to Equation 3 does not reflect a poorer fit to the data (cf. $s = 0.40$ vs. 0.41); rather it reflects the fact that a substantial source of variation in the permeability data has been removed by dividing P by the aqueous diffusivity D_0. We examined several possible dependencies of normalized permeability on solute size. The one shown in Equation 4 is among the best alternatives; however it should not be construed as representing a fundamental relationship. It can be seen from the regression that the size variable captures only slightly more than half of the residual variance in this dataset ($r^2 = 0.57$). Either there is another solute-related factor in play or the variability in nail plate permeability is indeed substantial. We noted in the course of this analysis that normalization of the permeability coefficients k_p' by thickness h to compute P failed to improve the correlation with molecular size, despite a factor of three variation in h (Table 1). This may, in fact, reflect the possibility that thicker nails have higher specific permeability, as might be expected for nails impacted by onychomycosis.

But let us return to the conditions under which the in vitro experiments were conducted and the four excluded solutes. Permeability data for these highly lipophilic (Figure 1a) compounds lie well above the regression lines in Figures 1 and 2. They come from three different sources (6, 8, 17). The results for ketoconazole (5) were obtained in our laboratory using solvent-deposited [3H]-ketoconazole. Normalized permeability was estimated by dividing the steady-state flux for the highest hydration state ($0.527\ \mu g \cdot cm^2 h^{-1}$) by the estimated water solubility value of $10.6\ \mu g \cdot cm^{-3}$, then multiplying by the nail thickness of 0.05 cm. It seems the results can be appropriately compared to liquid immersion studies, although tritium exchange (leading to a slow production of ^3H_2O) cannot be ruled out as a contributor to the measured flux. Similarly the results of Walters et al. (8) for decanol and dodecanol were also obtained with radiolabeled solutes, although in this case the label was ^{14}C. Perhaps there was an issue with radiochemical purity, but this hypothesis cannot be checked. The measurements, to our knowledge, have never been repeated. Finally, Kobayashi et al.'s results with flurbiprofen were obtained in a study which also included 5-fluorouracil (17). Both compounds were analyzed by HPLC, yet only one is found to be an outlier in the present dataset. Although it can be shown that approximately 40% of the flurbiprofen would have been ionized under the dose conditions employed in this study,

partial ionization would, if anything, have led to a lower observed permeability than that for the neutral compound (1). Thus, there is no readily apparent reason to discount the flurbiprofen data.

Other concerns with the present nail permeability data set may be raised. The Kobayashi group used diffusion cells with a very small aperture (0.049 cm^2) to study human nail clippings (1, 17). Assuming a circular geometry and the nail thickness of 0.04 cm reported by this group, an aspect ratio (thickness/radius) of 0.32 can be readily calculated. The influence of lateral diffusion in such cases can be significant and dependent upon the total size of the membrane relative to the exposed surface (18). Prior to achievement of a steady state, lateral diffusion reduces the flux through the membrane (18). The time lag to achieve steady state increases. But flux eventually increases beyond that expected in the absence of edge effects due to the larger effective cross sectional area for diffusion (19, 20). For an aspect ratio of 0.32 and a total nail clipping radius more than 20% greater than the exposed radius, one would expect an 8% *increase* in steady state flux relative to a large, planar sample according to the analysis of Barrer et al. (19), later summarized by Crank (20). Thus, edge effects could lead systematic errors in either direction in the permeability values reported by Kobayashi et al. (1, 17), depending on whether or not a true steady state was achieved. Achievement of steady state transport may also be prolonged by slow binding kinetics in a manner not easily detected by the investigator (21). However, none of these potential systematic errors seem to account for the 10- to 30-fold difference between the nail permeability data and the UB/UC theory. Furthermore, there are no systematic differences between the Kobayashi data and those obtained by other groups (Figure 2), other than the outlying data already discussed.

Finally, we note that hydrated hoof and horn permeabilities are higher than those in human nail plate, despite their similar water contents. To illustrate this point we have included the bovine hoof data for uncharged solutes from Mertin and Lippold (2) on the graph shown in Figure 2. These data lie well above the nail plate values, yet the fiber volume fraction we infer from this report is 0.58, comparable to that in nail. They overlap with three of the four excluded permeability values for nail plate and they lie close to the predictions of the UB/UC fiber matrix model. This comparison suggests that there is additional structure to the nail plate not included in the fiber matrix model that leads to lower permeability for hydrophilic to moderately lipophilic solutes. The most likely components to produce such an effect are the residual lipids, the concentrations of which are spatially dependent and average just below 1% of the overall nail composition (7). We postulate that remnants of cell membranes may form a discontinuous lipid barrier that partially impedes the diffusion of hydrophilic solutes.

Conclusions

There is still considerable uncertainty in the permeability characteristics of human nail plate, including the possible presence of a residual lipid barrier that impedes the permeation of polar solutes. Current diffusion models based on hydrogel analogies fail to adequately describe nail plate permeability, although one (UB/UC) may provide a reasonable representation for bovine hoof. The CAU model severely under predicts the permeability of

either nail or hoof, raising concerns regarding its merit for estimating corneocyte permeability in human stratum corneum.

Acknowledgments

Appendix

The diffusion theories embodied in the UB/UC (9, 12) and CAU (13) models combine elements of hydrodynamic theory and obstruction (steric) theory to describe the diffusion process in the corneocyte phase of the stratum corneum. They are based on established methods which factor in the hindrance effects due to hydrodynamic drag on the diffusing solute and steric effects due to volume excluded by the fiber fraction of the matrix. The effective diffusivity (D_e) of an uncharged solute molecule is described by a factorization of the form

$$\frac{D_e}{D_0} = f(\text{steric}) \cdot f(\text{hydro}) \quad \text{(A-1)}$$

where f(steric) is the steric reduction factor, f(hydro) is the hydrodynamic reduction factor and D_0 is the free diffusivity in aqueous solution. In order to describe also the reduction in permeability, $P = D_e \cdot K$, rather than just that in diffusivity, a second steric factor for the partition coefficient, K, must be inserted (9). Thus, for both models,

$$\frac{P}{D_0} = K \cdot f(\text{steric}) \cdot f(\text{hydro}) \quad \text{(A-2)}$$

UB/UC model

The steric reduction factor is described in terms of the fiber volume fraction inaccessible to the center of the solute molecule (φ_f') as given by Equation A-3,

$$f(\text{steric}) = 1 - \varphi_f' = 1 - \varphi_f (1+\lambda)^2 \quad 0 \leq \lambda \leq 0.25 \quad \text{(A-3)}$$

where $\lambda = R_s/R_f$, R_s is the solute radius and R_f is the radius of keratin microfibrils (35 Å). The partition coefficient K has the same value as f(steric); thus, the factor $(1 - \varphi_f')$ appears as the square in the final formula.

The hydrodynamic reduction factor, f(hydro), derives from a stretched exponential model similar to that used by Clague and Phillips (22), as described by Wang et al. (9). A simple polynomial expression of this relationship for a fiber volume fraction of 0.64 was derived by (12):

$$f(\text{hydro } \lambda, 0.64) = 0.5224\lambda^3 + 1.2776\lambda^2 - 2.5332\lambda + 1.0002 \quad \text{(A-4)}$$

$$\ldots\ldots\ldots 0 \le \lambda \le 0.5$$

Combining these results yields, for the UB/UC model,

$$\frac{P}{D_0} = \left(1 - \varphi_f'\right)^2 \cdot (0.5224\lambda^3 + 1.2776\lambda^2 - 2.5332\lambda + 1.0002) \quad \text{(A-5)}$$

$$\ldots\ldots\ldots 0 \le \lambda \le 0.25$$

CAU model

The CAU model was derived from a fiber matrix model originally developed for describing protein diffusion in an agarose gel (16). The steric hindrance factor is given by

$$f(\text{steric}) = \exp\left(-\alpha S^\delta\right) \quad \text{(A-6)}$$

$$S = \varphi_f (1+\lambda)^2 \quad \text{(A-7)}$$

where $\delta = 1.09$ (13, 16) and λ has the same meaning as in Equation A-3. The variable S may thus be seen to be equivalent to φ_f' in Equation A-3. The value $\alpha = 9.47$ was derived by fitting the model to skin permeability data of eight representative solutes (13).

The hydrodynamic hindrance offered by the fiber matrix was defined in terms of solute radius, R_s, and hydraulic permeability, κ, of the fibrous media; thus,

$$f(\text{hydro}) = \left[1 + \frac{R_s}{\sqrt{\kappa}} + \frac{R_s^2}{3\kappa}\right]^{-1} \quad \text{(A-8)}$$

$$\kappa = \beta R_f^2 \varphi_f^\gamma \quad \text{(A-9)}$$

where $\gamma = -1.17$ (13, 16). The value of κ was estimated as in (16) with the exception that the value $\beta = 9.32 \times 10^{-8}$ was derived by fitting the final model to the skin permeability data of eight representative solutes (13).

Combining the above results yields, for the CAU model,

$$\frac{P}{D_0} = \frac{\exp\,(-\alpha S^\delta).(1 - S)}{\left[1 + \frac{R_s}{\sqrt{\kappa}} + \frac{R_s^2}{3\kappa}\right]} \qquad \text{(A-10)}$$

References

1. Kobayashi Y, Komatsu T, Sumi M, Numajiri S, Miyamoto M, Kobayashi D, Sugibayashi K, Morimoto Y. In vitro permeation of several drugs through the human nail plate: relationship between physicochemical properties and nail permeability of drugs. Eur J Pharm Sci. 2004; 21:471–477. [PubMed: 14998577]

2. Mertin D, Lippold B. In vitro permeability of the human nail and a keratin membrane from bovine hooves: Prediction of the penetration rate of antimycotics through the nail plate and their efficacy. J Pharm Pharmacol. 1997; 49:866–872. [PubMed: 9306253]

3. Amsden B. Solute diffusion within hydrogels. Mechanisms and models. Macromolecules. 1998; 31:8382–8395.

4. Hao J, Li SK. Transungual iontophoretic transport of polar neutral and positively charged model permeants: effects of electrophoresis and electroosmosis. J Pharm Sci. 2008; 97:893–905. [PubMed: 17683062]

5. Gunt HB, Kasting GB. Equilibrium water sorption characteristics of the human nail. J Cosmet Sci. 2007; 58:1–9. [PubMed: 17342263]

6. Gunt HB, Kasting GB. Effect of hydration on in vitro permeation of ketoconazole through human nail plate. Eur J Pharm Sci. 2007; 32:254–260. [PubMed: 17928205]

7. Dawber, R., deBerker, D., Baran, R. Science of the nail apparatus. In: Baran, R., editor. Baran and Dawber's Diseases of the Nails and Their Management. Malden, MA: Blackwell Science; 2001. p. 1-47.

8. Walters KA, Flynn GL, Marvel JR. Physicochemical characterization of the human nail permeation pattern for water and the homologous alcohols and differences with respect to the stratum corneum. J Pharm Pharmacol. 1983; 35:28–33. [PubMed: 6131961]

9. Wang T-F, Kasting GB, Nitsche JM. A multiphase microscopic model for stratum corneum permeability. II. Estimation of physicochemical parameters and application to a large permeability database. J Pharm Sci. 2007; 96:3024–3051. [PubMed: 17876780]

10. Poling, BE., Prausnitz, JM., O'Connell, JP. The properties of gases and liquids. 5. New York: McGraw-Hill; 2001.

11. Hayduk W, Laudie H. Prediction of diffusion coefficients for nonelectrolytes in dilute aqueous solutions. AIChE J. 1974; 20:611–615.

12. Wang, T-F. Microscopic models for the structure and permeability of the stratum corneum barrier layer of skin [Ph.D.]. Buffalo: State University of New York; 2003.

13. Chen L, Lian G, Han L. Modeling transdermal permeation. Part I. Predicting skin permeability of both hydrophobic and hydrophilic solutes. AIChE J. 2010; 56:1136–1146.

14. Kasting, G., Nitsche, JM. Mathematical models of skin permeability: microscopic transport models and their predictions. In: Querleux, B., editor. Computational Biophysics of the Skin. Pan Stanford Publishing, Inc.; 2014. p. 187-216.

15. Phillips RJ, Dean WM, Brady JF. Hindered transport in fibrous membranes and gels: effect of solute size and fiber configuration. J Colloid Interface Sci. 1990; 139:363–373.

16. Johnson EM, Berk DA, Jain RK, Deen WM. Hindered diffusion in agarose gels: test of effective medium model. Biophys J. 1996; 70:1017–1026. [PubMed: 8789119]

17. Kobayashi Y, Miyamoto M, Sugibayashi K, Morimoto Y. Drug permeation through the three layers of the human nail plate. J Pharm Pharmacol. 1999; 51:271–278. [PubMed: 10344627]

18. Palliyil B, Li C, Owaisat S, Lebo D. Lateral drug diffusion in human nails. AAPS PharmSciTech. 2014:1–10. [PubMed: 24022347]

19. Barrer R, Barrie J, Rogers M. Permeation through a membrane with mixed boundary conditions. Trans Faraday Soc. 1962; 58:2473–2483.

20. Crank, J. The Mathematics of Diffusion. 2nd. Clarendon Press; 1975. p. 64-65.

21. Frasch HF, Barbero AM, Hettick JM, Nitsche JM. Tissue binding affects the kinetics of theophylline diffusion through the stratum corneum barrier layer of skin. Journal of Pharmaceutical Sciences. 2011; 100:2989–2995. [PubMed: 21283983]

22. S Clague, D., J Phillips, R. Hindered diffusion of spherical macromolecules through dilute fibrous media. Melville, NY, ETATS-UNIS: American Institute of Physics; 1996.

23. Malhotra GG, Zatz JL. Investigation of nail permeation enhancement by chemical modification using water as a probe. J Pharm Sci. 2002; 91:312–323. [PubMed: 11835191]

24. Malhotra GG, Zatz JL. Characterization of the physical factors affecting nail permeation using water as a probe. J Cosmet Sci. 2000; 51:367–377.

25. Walters KA, Flynn GL, Marvel JR. Physicochemical characterization of the human nail: I. Pressure sealed apparatus for measuring nail plate permeabilities. J Invest Dermatol. 1981; 76:76–79. [PubMed: 7462680]

26. Smith KA, Hao J, Li SK. Influence of pH on transungual passive and iontophoretic transport. J Pharm Sci. 2010; 99:1955–1967. [PubMed: 19904826]

27. Hao J, Smith KA, Li SK. Chemical method to enhance transungual transport and iontophoresis efficiency. Int J Pharm. 2008; 357:61–69. [PubMed: 18321669]

28. Hao J, Li SK. Mechanistic study of electroosmotic transport across hydrated nail plates: Effects of pH and ionic strength. J Pharm Sci. 2008; 97:5186–5197. [PubMed: 18386836]

29. Mertin D, Lippold BC. In-vitro permeability of the human nail and of a keratin membrane from bovine hooves: influence of the partition coefficient octanol/water and the water solubility of drugs on their permeability and maximum flux. J Pharm Pharmacol. 1997; 49:30–34. [PubMed: 9120766]

30. Murthy SN, Waddell DC, Shivakumar HN, Balaji A, Bowers CP. Iontophoretic permselective property of human nail. J Derm Sci. 2007; 46:150–152.

31. Smith KA, Hao J, Li SK. Effects of ionic strength on passive and iontophoretic transport of cationic permeant across human nail. Pharm Res. 2009; 26:1446–1455. [PubMed: 19267187]

32. Vejnovic I, Simmler L, Betz G. Investigation of different formulations for drug delivery through the nail plate. Int J Pharm. 2010; 386:185–194. [PubMed: 19941943]

33. Walters KA, Flynn GL, Marvel JR. Penetration of the human nail plate: the effects of vehicle pH on the permeation of miconazole. J Pharm Pharmacol. 1985; 37:498–499. [PubMed: 2863357]

34. Kasting GB, Barai ND, Wang T-F, Nitsche JM. Mobility of water in human stratum corneum. J Pharm Sci. 2003; 92:2326–2340. [PubMed: 14603517]

(a)

$y = -0.02\,x - 6.85$

$n = 38,\ s = 0.72,\ R^2 = 0.003$

log k_p'

log $K_{o/w}$

The graph plots $\log k_p{}'$ (y-axis, from -10 to -4) versus $\log MW$ (x-axis, from 1.0 to 3.0) with a linear fit:

$$y = -1.76\,x - 3.09$$

$$n = 38,\ s = 0.41,\ R^2 = 0.68$$
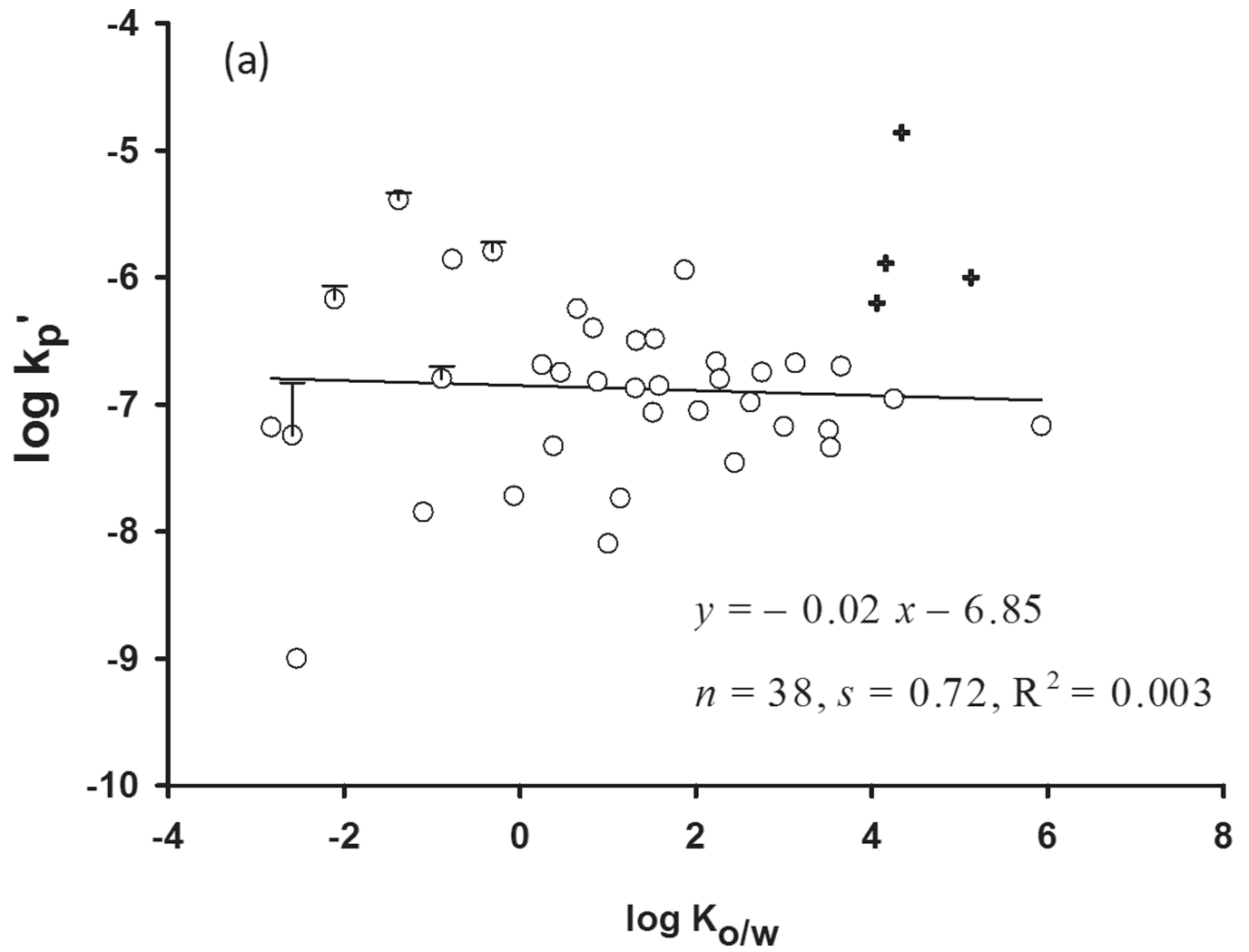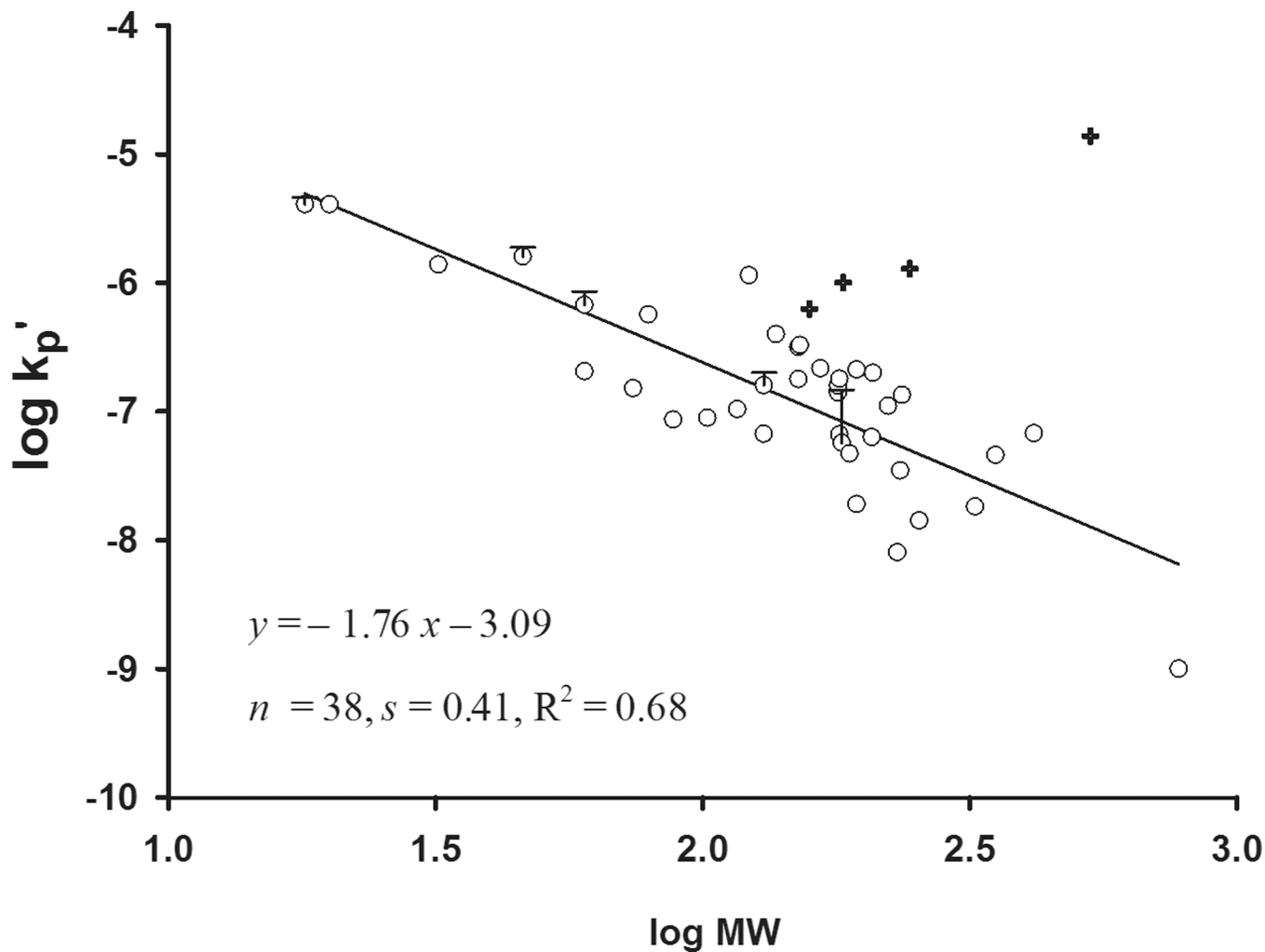
Figure 1.
Plot of (a) log of temperature-corrected nail permeability coefficient ($k_p{}'$) versus log octanol/water partition coefficient for the 42 solutes in Table 1; (b) log $k_p{}'$ versus log molecular weight for the same dataset. Mean values with upper error bars (+1 SD) are displayed for repeated measurements. The four solutes plotted as + symbols were excluded from the analysis as described in the text.
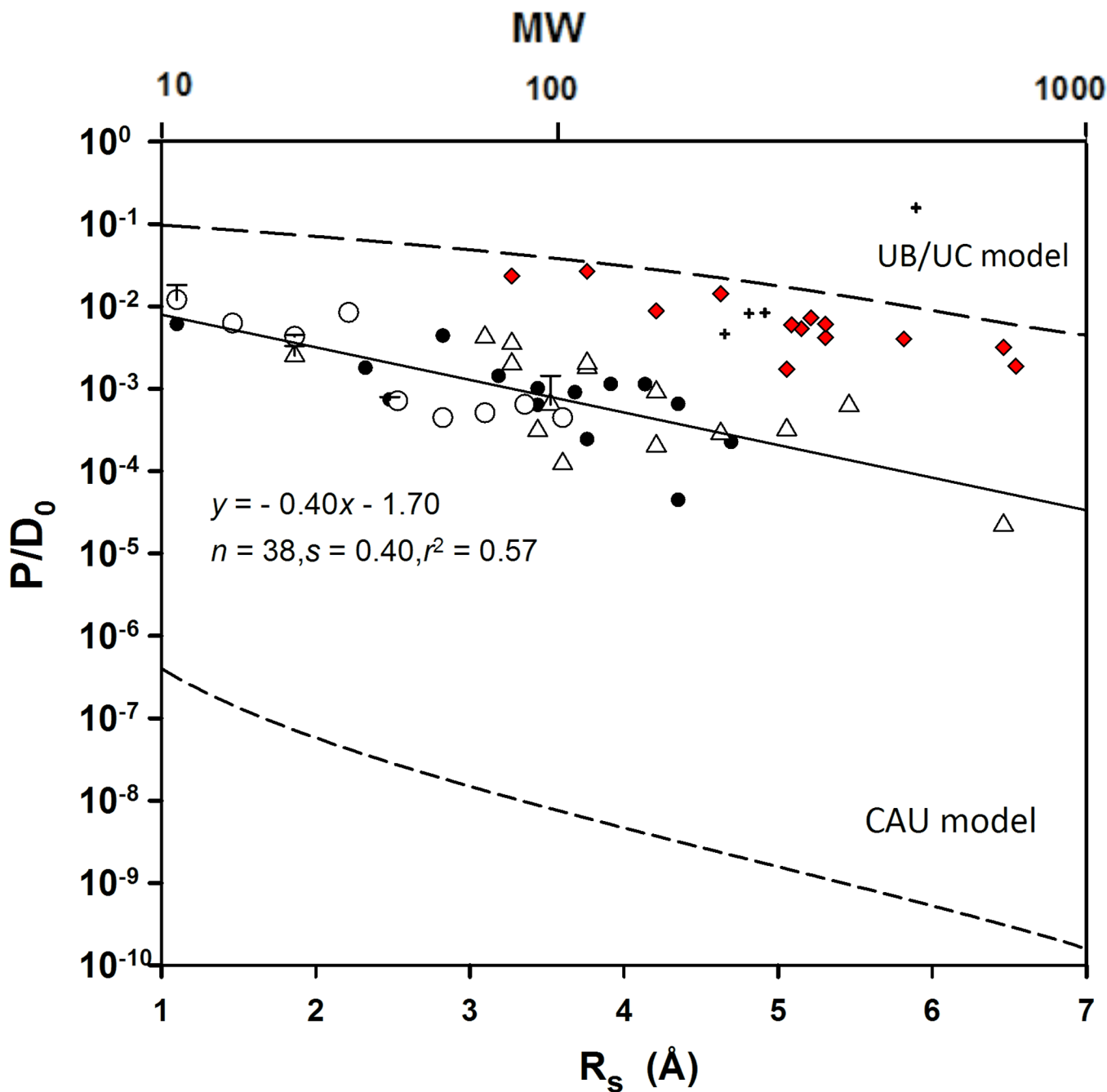
Figure 2.
Specific permeability $P = D \cdot K$ of human nail plate to uncharged solutes, normalized by their estimated diffusivities D_0 in aqueous solution, plotted versus the solute radius, R_s. ● Kobayashi et al. (1, 17); ○ Walters et al. (8, 25, 33);   Other sources; + Excluded data; ◆ Bovine hoof data from Mertin and Lippold (2). Upper error bars (+1 SD) are displayed for repeated measurements. Shown for comparison are the predictions of two fiber matrix diffusion models developed for the corneocyte phase of partially hydrated human stratum corneum, which has approximately the same water content as hydrated nail plate. A keratin

fiber radius of 35 Å has been assumed for both calculations. The UB/UC model overestimates the permeability, while the CAU model severely underestimates permeability.

Table 1

Physicochemical properties and permeability coefficients of 42 uncharged compounds in nail plate.

Compound	MW Da	$\log K_{o/w}$ [a]	R_s [b] Å	$D_0 \times 10^6$ cm²/s	T °C	h cm	$k_p \times 10^7$ cm/s	$k_p' \times 10^7$ cm/s	$P \times 10^8$ cm²/s	Reference
Water	18	−1.38	1.10	26.6	37	0.121	51.3[c]	45.7	55.3	(23)
					37	0.050[d]	38.1[c]	33.9	17.0	(24)
					37	0.063	45.8	40.8	25.7	(8, 25)
					20	0.070	31	42	30	(26)
Deuterium oxide	20	−1.38	1.10	26.6	37	0.040	45.52	40.51	16.21	(1)
Methanol	32	−0.77	1.46	20.0	37	0.091	16	14	13	(8, 25)
Ethanol	46	−0.31	1.86	15.7	37	0.046	16	14	6.5	(8, 25)
					37	0.040	19.81	17.63	7.040	(1)
n-Propanol	60	0.25	2.21	13.2	37	0.054	2.3	2.1	1.1	(8)
Urea	60	−2.11	1.86	15.7	20	0.055	3.8[e]	5.1	2.8	(4)
					20	0.065	6.0[c]	8.2	5.3	(27)
					20	0.055	5	7	4	(28)
n-Butanol	74	0.88	2.53	11.5	37	0.054	1.7	1.5	0.82	(8)
Pyridine	79	0.65	2.32	12.6	37	0.040	6.36	5.66	2.26	(1)
n-Pentanol	88	1.51	2.82	10.3	37	0.054	0.97	0.86	0.46	(8)
n-Hexanol	102	2.03	3.10	9.43	37	0.054	1.00	0.89	0.48	(8)
n-Heptanol	116	2.62	3.36	8.71	37	0.054	1.17	1.04	0.56	(8)
Benzoic acid	122	1.87	2.82	10.3	37	0.040	12.84	11.43	4.571	(1)
5-Fluorouracil	130	−0.89	2.48	11.8	37	0.040	2.08	1.85	0.74	(1)
					37	0.049	1.49	1.33	0.65	(17)
n-Octanol	130	3.00	3.60	8.11	37	0.054	0.75	0.67	0.36	(8)
Methyl nicotinate	137	0.83	3.10	9.43	32	0.100	3.98[c]	3.98	3.98	(29)
Paracetamol	150	0.46	3.27	8.93	32	0.100	1.78	1.78	1.78	(2)
Ethyl nicotinate	151	1.32	3.27	8.93	32	0.100	3.16[c]	3.16	3.16	(29)
Methyl paraben	152	1.53	3.19	9.17	37	0.040	3.68	3.28	1.31	(1)
n-Decanol [f]	158	4.06	4.06	7.19	37	0.054	6.9	6.2	3.3	(8)

Compound	MW Da	log $K_{o/w}$ [a]	R_s [b] Å	$D_0 \times 10^6$ cm²/s	T °C	h cm	$k_p \times 10^7$ cm/s	$k_p' \times 10^7$ cm/s	$P \times 10^8$ cm²/s	Reference
Ethyl paraben	166	2.23	3.44	8.49	37	0.040	2.43	2.16	0.86	(1)
Phenacetin	179	1.58	3.76	7.77	32	0.100	1.40	1.40	1.40	(2)
Butyl nicotinate	179	2.27	3.76	7.77	32	0.100	1.58[c]	1.58	1.58	(29)
Propyl paraben	180	2.75	3.68	7.94	37	0.040	2.01	1.79	0.72	(1)
Glucose	180	−3.24	3.44	8.49	25	0.040	0.6[c]	0.7	0.3	(30)
Mannitol	182	−2.59[e]	3.52	8.30	20	0.055	0.5	0.7	0.4	(28)
					20	0.065	0.30	0.41	0.27	(27)
					20	0.055	0.24[e]	0.32	0.18	(4)
					20	0.055	0.18[e]	0.24	0.13	(4)
					20	0.065	2.0[g]	2.7	1.7	(31)
n-Dodecanol [f]	183	5.13	4.49	6.51	37	0.054	11	10	5.5	(8)
Antipyrine	188	0.38	3.76	7.77	37	0.040	0.53	0.47	0.19	(1)
Caffeine	194	−0.07	3.60	8.11	32	0.050[d]	0.19[c]	0.19	0.10	(32)
Butyl paraben	194	3.13	3.91	7.47	37	0.040	2.38	2.12	0.85	(1)
Hexyl nicotinate	207	3.51	4.21	6.94	32	0.100	0.63[c]	0.63	0.63	(29)
Pentyl paraben	208	3.65	4.14	7.06	37	0.040	2.24	1.99	0.80	(1)
Hexyl paraben	222	4.25	4.35	6.71	37	0.040	1.24	1.10	0.44	(1)
Aminopyrine	231	1.00	4.35	6.71	37	0.040	0.09	0.08	0.03	(1)
Lidocaine	234	2.44	4.70	6.22	37	0.040	0.39	0.35	0.14	(1)
Isosorbide dinitrate	236	1.31	3.44	8.49	37	0.040	1.51	1.34	0.54	(1)
Flurbiprofen [f]	248	4.16	4.32	6.77	37	0.043	14.5	12.9	5.55	(17)
Diprophylline	254	−1.10	4.21	6.94	32	0.100	0.142	0.142	0.142	(2)
Chloramphenicol	323	1.14	4.63	6.31	32	0.100	0.182	0.182	0.182	(2)
Griseofulvin	353	3.53	5.06	5.78	25	0.040	0.4[c]	0.5	0.2	(30)
Miconazole	416	5.93	5.46	5.35	37	0.050[d]	0.75[c]	0.67	0.34	(33)
Ketoconazole [f]	531	3.55	6.54	4.47	32	0.051	138[c]	138	70.4	(6)
Iopamidol	777	−2.54	6.46	4.52	32	0.100	0.010	0.010	0.010	(2)

[a] Experimental values preferred when available or else predicted ACD log $K_{o/w}$ values were used from www.chemspider.com

[b]Radius calculated by Schroeder's method (10). For H_2O and D_2O, R_S=1.10 Å (34)

[c]Read from graph and/or calculated from reported (or read from graph) flux values and concentration

[d]Assumed thickness of 0.05 cm

[e]Average of 3 sets of different experiments

[f]Solutes excluded from the analysis

[g]Average of 2 sets of different experiments